Proceedings of *RAGtime 17–19, 17–19/23–26 Oct., 1–5 Nov., 2015/2016/2017, Opava, Czech Republic*
Z. Stuchlík, G. Török and V. Karas, editors, Silesian University in Opava, 2017, pp. 177–193

A one-parametric formula relating the frequencies of twin-peak quasi-periodic oscillations

Gabriel Török[1,a] Kateřina Goluchová[1] Eva Šrámková[1]
Jiří Horák[2] Pavel Bakala[1] and Martin Urbanec[1]

[1] Institute of Physics and Research Centre for Computational Physics and Data Processing, Faculty of Philosophy & Science, Silesian University in Opava, Bezručovo nám. 13, CZ-746 01 Opava, Czech Republic
[2] Astronomical Institute, Boční II 1401/2a, CZ-14131 Praha 4 - Spořilov, Czech Republic
[a] gabriel.torok@gmail.com

ABSTRACT
Timing analysis of X-ray flux in more than a dozen low-mass X-ray binary systems containing a neutron star reveals remarkable correlations between frequencies of two characteristic peaks present in the power-density spectra. We find a simple analytic relation that well reproduces all these individual correlations. We link this relation to a physical model which involves accretion rate modulation caused by an oscillating torus.

Keywords: X-Rays: Binaries — Accretion, Accretion Disks — Stars: Neutron

1 INTRODUCTION

Low-mass X-ray binaries (LMXBs) provide a unique opportunity to probe the effects associated with strong gravity. The way electromagnetic radiation propagates in space, its time variability, and shape of lines in its energetic spectrum, are all invaluable tools for exploring physical behaviour of matter in strong gravitational field around black holes (BHs) and neutron stars (NSs). A systematic study of NS properties similarly allows for exploration of the supra-dense matter (Lewin et al., 1997).

High-frequency quasi-periodic oscillations (HF QPOs) appear in the X-ray flux of several LMXBs. In NS sources they commonly occur in pairs, therefore being called twin-peak HF QPOs (van der Klis, 2006). The Rossi X-ray timing explorer (RXTE Bradt et al., 1993), which operated from 1995 to 2012, has provided a large amount of NS data. Timing analysis of the X-ray flux in more than a dozen NS systems reveals remarkable correlations between frequencies of two characteristic peaks present in the power-density spectra. In Figure 1 we illustrate these correlations in terms of the upper and lower QPO frequency, ν_U and ν_L, for a group of 14 sources. The Figure comprehends a major part of the available twin-peak QPO measurements in 8 atoll sources, 5 Z sources, and one mili-second X-ray

978-80-7510-257-7

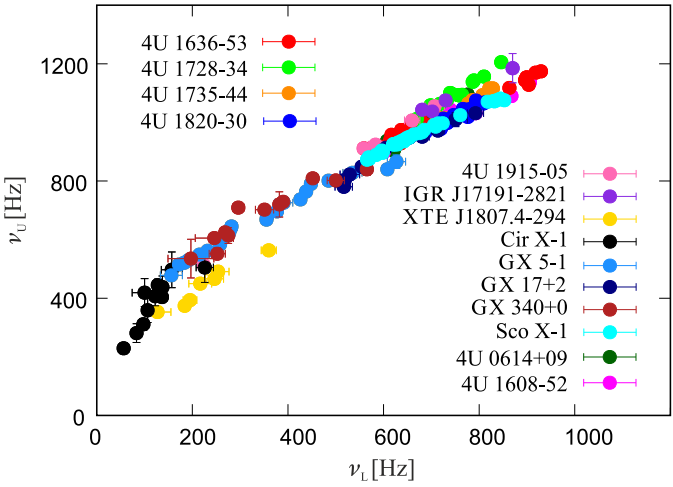

Figure 1. Correlations between frequencies of twin-peak QPOs observed in 14 sources. Properties of these sources and relevant references are given in Table 1.

pulsar (see Table 1 for the list of sources and references). A great number of various theories has been proposed to explain the observed phenomenon. Most often, QPOs are related to orbital motion in strong gravity. Many astrophysicists believe that observations of QPOs may be beneficial in studying the properties of NSs and strong gravitational field, e.g., utilizing QPO frequency correlations (Alpar and Shaham, 1985; Lamb et al., 1985; Miller et al., 1998; Psaltis et al., 1999; Stella and Vietri, 2001; Wagoner et al., 2001; Kluźniak and Abramowicz, 2001; Kato, 2001; Titarchuk and Wood, 2002; Abramowicz et al., 2003; Rezzolla et al., 2003; Kluźniak et al., 2004; Zhang, 2004; Pétri, 2005; Bursa, 2005; Čadež et al., 2008; Mukhopadhyay, 2009; Stuchlík et al., 2013).

2 A ONE-PARAMETRIC RELATION

Up to this date most researchers have been unsuccessful in their attempt to model the individual observed correlations using simple formulae based on geodesic orbital motion (e.g., Lin et al., 2011; Török et al., 2016b and references therein).

2.1 Physical arguments for one-parametric relation

In the series of works (Török et al., 2010, 2012, 2016b) the authors discussed the effective degeneracy between various parameters of the relativistic precession (RP) model as well as several other orbital QPO models. Within this degeneracy, each combination of NS mass M, angular momentum j and quadrupole moment q corresponds to a certain value of

Table 1. List of sources and references, and parameters resulting from matching the observed correlations between twin-peak QPO frequencies by the linear relation, $\nu_U = a\nu_L + b$. The goodness of fits is formally characterized by the χ^2 values. The uncertainties displayed here correspond to standard errors.

Source No./ Type[a]	Name	a	$b[Hz]$	$\frac{\chi^2_{lin}}{d.o.f.}$	Data-points
1/A	4U 1608-52	$0.75^{\pm 0.01}$	$458^{\pm 6}$	30	12
2/A	4U 1636-53	$0.72^{\pm 0.01}$	$505^{\pm 3}$	35	22
3/A	4U 1735-44	$0.91^{\pm 0.01}$	$362^{\pm 4}$	6	8
4/A	4U 1915-05	$1.15^{\pm 0.01}$	$256^{\pm 4}$	1	5
5/A	IGR J17191-2821	$0.73^{\pm 0.02}$	$540^{\pm 10}$	1	4
6/Z	GX 17+2	$0.90^{\pm 0.02}$	$342^{\pm 9}$	10	10
7/Z	Sco X-1	$0.75^{\pm 0.01}$	$456^{\pm 1}$	85	39
8/Z	Cir X-1	$2.39^{\pm 0.14}$	$97^{\pm 16}$	11	11
9/P	XTE J1807.4-294	$1.10^{\pm 0.05}$	$183^{\pm 12}$	5	7
10/A	4U 1728-34	$0.97^{\pm 0.01}$	$370^{\pm 5}$	37	15
11/A	4U 0614+09	$1.02^{\pm 0.1}$	$303^{\pm 4}$	11	13
12/A	4U 1820-30	$0.89^{\pm 0.01}$	$353^{\pm 2}$	74	23
13/Z	GX 340+0	$0.84^{\pm 0.04}$	$402^{\pm 14}$	23	12
14/Z	GX 5-1	$0.86^{\pm 0.02}$	$372^{\pm 7}$	49	21

[a] A - atoll, Z - Z, P - pulsar.

References: (1)–(3), (10) – (12) - Barret et al. (2005a,b, 2006), (4) - Boirin et al. (2000), (5) - Altamirano et al. (2010), (6) - Homan et al. (2002), (7) - van der Klis et al. (1997), (8) - Boutloukos et al. (2006), (9) - Linares et al. (2005), (13) - Jonker et al. (2000), (14) - Jonker et al. (2002).

a single generalized parameter $\mathcal{M}$, e.g., non-rotating NS mass. This degeneracy seems to be a generic property of geodesic QPO models,

$$\nu_L = \nu_L(\nu_U, \mathcal{M}), \; \nu_U = \nu_U(\nu_L, \mathcal{M}). \tag{1}$$

2.2 Observational evidence of one-parametric relation

Fitting of QPO frequencies with ad-hoc (phenomenological) relations has been discussed in a number of studies. In several cases the fits are reliable when two free parameters specific for each source are considered (e.g., Psaltis et al., 1998; Abramowicz et al., 2005b,a; Zhang et al., 2006). We investigate parameters of various fitting relations and find that these parameters are strongly correlated.

It has been noticed by Abramowicz et al. (2005a,b) that the slope a and intercept b of the linear fits ($\nu_U = a\nu_L + b$) are roughly related as $a \approx 1.5 - 0.0015b$. We find that similar behaviour arises for the quadratic relation, $\nu_U = a\nu_L^2 + b$, the square-root relation, $\nu_U = a\sqrt{\nu_L} + b$, and the power-law relation $\nu_U = b(1\nu_L)^a$. Detailed outcomes of data fitting are shown in Tables 1–4 and illustrated in Figure 2.

Table 2. Parameters resulting from matching the observed correlations between twin-peak QPO frequencies by the quadratic relation, $\nu_U = a\nu_L^2 + b$.

Source No./ Type	Name	$a \times 10^4$	$b[Hz]$	$\frac{\chi^2}{d.o.f.}$	Data-points
1/A	4U 1608-52	$5.3^{\pm 0.2}$	$716^{\pm 4}$	45	12
2/A	4U 1636-53	$4.8^{\pm 0.1}$	$764^{\pm 3}$	44	22
3/A	4U 1735-44	$5.9^{\pm 0.1}$	$712^{\pm 3}$	5	8
4/A	4U 1915-05	$13.7^{\pm 0.8}$	$445^{\pm 7}$	8	5
5/A	IGR J17191-2821	$4.9^{\pm 0.2}$	$811^{\pm 9}$	1	4
6/Z	GX 17+2	$7.5^{\pm 0.3}$	$607^{\pm 11}$	17	10
7/Z	Sco X-1	$5.5^{\pm 0.1}$	$708^{\pm 3}$	211	39
8/Z	Cir X-1	$121.3^{\pm 15.8}$	$202^{\pm 19}$	17	11
9/P	XTE J1807.4-294	$22.9^{\pm 2.8}$	$305^{\pm 12}$	8	7
10/A	4U 1728-34	$6.6^{\pm 0.1}$	$725^{\pm 5}$	36	15
11/A	4U 0614+09	$7.5^{\pm 0.1}$	$647^{\pm 4}$	12	13
12/A	4U 1820-30	$6.2^{\pm 0.1}$	$671^{\pm 2}$	74	23
13/Z	GX 340+0	$11.1^{\pm 1.2}$	$551^{\pm 12}$	36	12
14/Z	GX 5-1	$12.1^{\pm 1.0}$	$505^{\pm 12}$	160	21

Table 3. Parameters resulting from matching the observed correlations between twin-peak QPO frequencies by the square-root relation, $\nu_U = a\sqrt{\nu_L} + b$.

Source No./ Type	Name	a	$b[Hz]$	$\frac{\chi^2}{d.o.f.}$	Data-points
1/A	4U 1608-52	$40^{\pm 1}$	$-71^{\pm 6}$	26	12
2/A	4U 1636-53	$40^{\pm 1}$	$-47^{\pm 3}$	37	22
3/A	4U 1735-44	$51^{\pm 1}$	$-352^{\pm 6}$	6	8
4/A	4U 1915-05	$46^{\pm 1}$	$-175^{\pm 3}$	1	5
5/A	IGR J17191-2821	$40^{\pm 1}$	$-7^{\pm 10}$	2	4
6/Z	GX 17+2	$45^{\pm 1}$	$-217^{\pm 8}$	8	10
7/Z	Sco X-1	$39^{\pm 1}$	$-50^{\pm 2}$	51	39
8/Z	Cir X-1	$47^{\pm 2}$	$-127^{\pm 14}$	10	11
9/P	XTE J1807.4-294	$35^{\pm 1}$	$-90^{\pm 11}$	4	7
10/A	4U 1728-34	$53^{\pm 1}$	$-354^{\pm 5}$	37	15
11/A	4U 0614+09	$53^{\pm 1}$	$-383^{\pm 4}$	12	13
12/A	4U 1820-30	$51^{\pm 1}$	$-377^{\pm 2}$	73	23
13/Z	GX 340+0	$32^{\pm 1}$	$102^{\pm 12}$	19	12
14/Z	GX 5-1	$32^{\pm 1}$	$85^{\pm 6}$	30	21

These findings imply that (the one) relation between the QPO frequencies should be based mostly on a single $\mathcal{M}$ parameter.

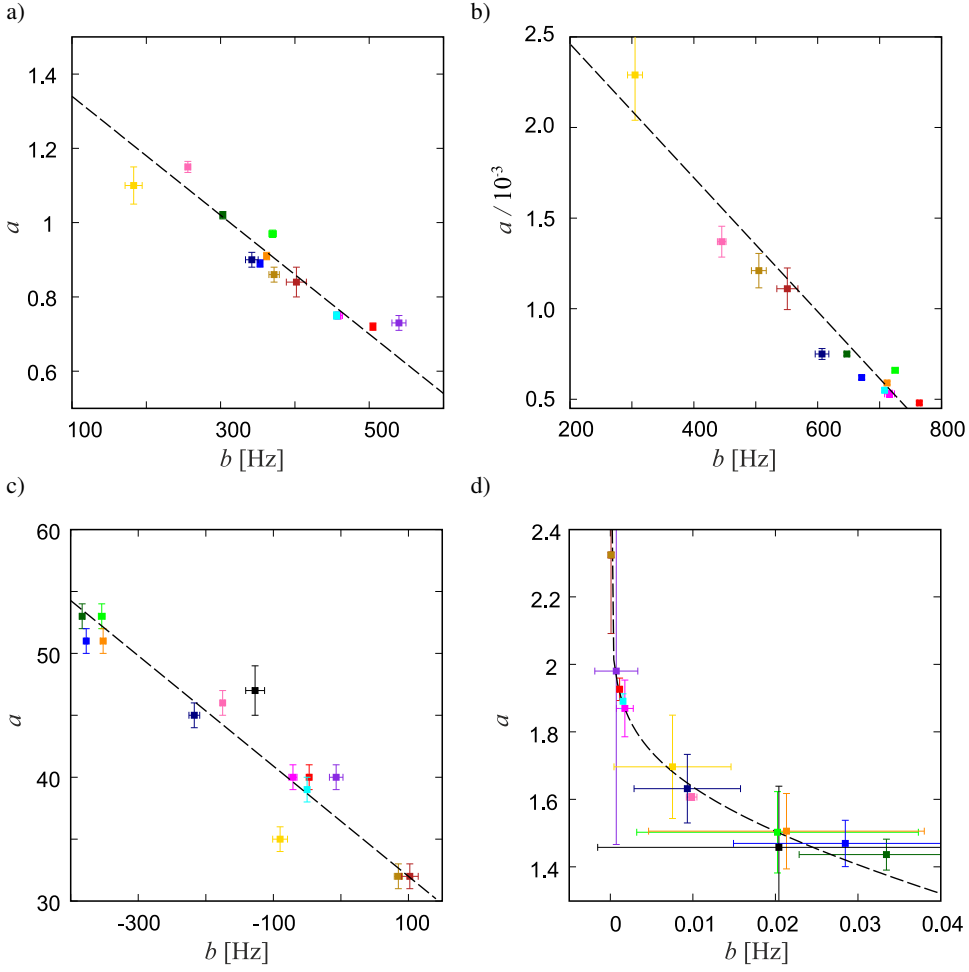

Figure 2. The fitting relations parameters obtained for the individual sources. a) The linear relation. b) The quadratic relation. c) The square-root relation. d) The power-law relation. In all the four panels the dashed line indicates the character of the $a(b)$ dependence.

Table 4. Parameters resulting from matching the observed correlations between twin-peak QPO frequencies by the power-law relation, $\nu_U = b(1\nu_L)^a$.

Source No./ Type	Name	a	$b[Hz]$	$\frac{\chi^2}{d.o.f.}$	Data-points
1/A	4U 1608-52	$0.0018^{\pm 0.0010}$	$1.87^{\pm 0.0841}$	20	12
2/A	4U 1636-53	$0.0011^{\pm 0.0003}$	$1.93^{\pm 0.0332}$	35	22
3/A	4U 1735-44	$0.0213^{\pm 0.0167}$	$1.51^{\pm 0.1118}$	6	8
4/A	4U 1915-05	$0.0099^{\pm 0.0006}$	$1.61^{\pm 0.0101}$	1	5
5/A	IGR J17191-2821	$0.0007^{\pm 0.0026}$	$1.98^{\pm 0.5138}$	1	4
6/Z	GX 17+2	$0.0093^{\pm 0.0064}$	$1.63^{\pm 0.1015}$	8	10
7/Z	Sco X-1	$0.0015^{\pm 0.0002}$	$1.89^{\pm 0.0220}$	51	39
8/Z	Cir X-1	$0.0204^{\pm 0.0219}$	$1.46^{\pm 0.1812}$	10	11
9/P	XTE J1807.4-294	$0.0075^{\pm 0.0071}$	$1.70^{\pm 0.1531}$	4	7
10/A	4U 1728-34	$0.0203^{\pm 0.0171}$	$1.50^{\pm 0.1205}$	32	15
11/A	4U 0614+09	$0.0335^{\pm 0.0106}$	$1.44^{\pm 0.0458}$	11	13
12/A	4U 1820-30	$0.0285^{\pm 0.01355}$	$1.47^{\pm 0.0686}$	69	23
13/Z	GX 340+0	$0.0001^{\pm 0.0001}$	$2.32^{\pm 0.2325}$	18	12
14/Z	GX 5-1	$0.0001^{\pm 0.0001}$	$2.32^{\pm 0.0073}$	29	21

3 GLOBAL MODES OF ACCRETED FLUID MOTION

Török et al. (2016a) explored a model of an oscillating torus. In this model (in next referred to as the CT model), the torus is assumed to form a cusp by filling up the critical equipotential volume. The observed HF QPO frequencies are here identified with the frequencies of global modes of the accreted fluid motion. The upper HF QPO frequency is assumed to be the Keplerian orbital frequency of the fluid defined at the centre of the torus where both pressure and density peak, and from which most of the torus radiation emerges. The lower HF QPO corresponds to the non-axisymmetric $m = -1$ radial epicyclic mode. Overall, we may write

$$\nu_U \equiv \nu_K(r_0), \tag{2}$$

$$\nu_L \equiv \nu_{\mathrm{r},-1}(r_0, \beta). \tag{3}$$

The QPO frequencies therefore strongly depend on the position of the centre of the torus r_0 and its thickness β. The configuration of a torus with cusp is defined by

$$\beta(r_0) \doteq \beta_{\mathrm{c}}(r_0). \tag{4}$$

In other words, we expect that for a given r_0 the torus is always close to its maximal possible size filling its 'Roche-like' lobe (see Figure 3 for illustration). For a given accreting central compact object our model predicts that the QPO frequencies are functions of a sin-

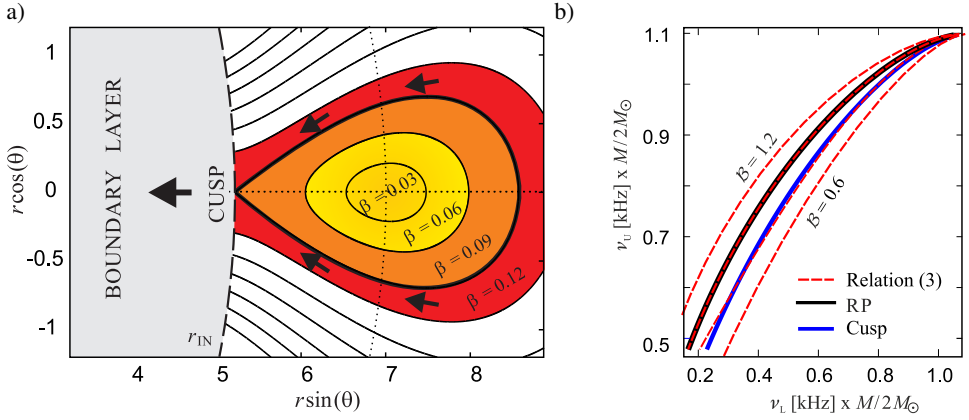

Figure 3. The CT model and its relation to formula (9). The β (panel a) and $\mathcal{B}$ (panel b) symbols denote different physical quantities. a) An illustration of equipotential surfaces of an accretion torus. The yellow colour denotes a non-accreting equilibrium torus. The thick black curve which bounds the orange region signifies the critical equipotential surface corresponding to a torus with cusp. b) A comparison between shapes of the $\nu_U(\nu_L)$ curves predicted by the RP model (the black line), CT model (the blue line) and relation (9) for $\mathcal{B} \in \{0.6,\ 0.8,\ 1.0,\ 1.2\}$ (the dashed red lines). The RP model curve coincides with those given by relation (9) for $\mathcal{B} = 1$ while the CT model curve nearly overlaps with those given by relation (9) for $\mathcal{B} = 0.8$.

gle parameter r_0,

$$\nu_U \equiv \nu_K(r_0), \tag{5}$$

$$\nu_L \equiv \nu_{\mathrm{r},-1}\left[r_0, \beta_c(r_0)\right] . \tag{6}$$

Rather long analytic formulae that define $\nu_{\mathrm{r},-1}$ can be found in Straub and Šrámková (2009). In Török et al. (2016a) the authors numerically calculated the $\nu_L(\nu_U)$ correlation following from relations (5) and (6). Assuming this correlation they obtained good match of data in the case of the atoll source 4U 1636-53 for NS mass of $M_0 = 1.7 M_\odot$.

4 ANALYTIC RELATION THAT WELL MATCHES THE DATA

In Török et al. (2017) we have suggested that frequency relations $\nu_L(\nu_U)$ are scaled as

$$\nu_L = \nu_U \left(1 - \mathcal{B}\sqrt{1 - (\nu_U/\nu_0)^{2/3}}\right), \tag{7}$$

where ν_0 represents the highest possible QPO frequency, $\nu_0 \geq \nu_U \geq \nu_L$. For orbital QPO models, ν_0 is the characteristic frequency of the orbital motion. When ν_0 equals the Keplerian orbital frequency at the innermost stable circular orbit around a non-rotating NS

with gravitational mass M_0, it can be expressed in the units of Hz as (e.g., Kluzniak and Wagoner, 1985; Kluzniak et al., 1990)

$$\nu_0 = \nu_{ISCO} = \frac{1}{6^{3/2}} \frac{c^3}{2\pi G} \frac{1}{M} = 2198 \frac{M_\odot}{M_0} = 2198 \frac{1}{\mathcal{M}}. \tag{8}$$

Hence relation (7) can be written in the form

$$\nu_L = \nu_U \left(1 - \mathcal{B} \sqrt{1 - 0.0059 (\nu_U \mathcal{M})^{2/3}}\right). \tag{9}$$

For $\mathcal{B} = 1$, relation (9) merges with the frequency relation implied by the RP model. This is illustrated in Figure 3 where we plot the curve predicted by the RP model along with the curves given by relation (9) for $\mathcal{B} \in \{(0.6,\ 0.8,\ 1.0,\ 1.2\}$. In the same Figure we include the curve calculated using the CT model. One can see that the CT model prediction is well approximated by relation (9) for $\mathcal{B} = 0.8$,

$$\nu_L = \nu_U \left(1 - 0.8 \sqrt{1 - 0.0059 (\nu_U \mathcal{M})^{2/3}}\right). \tag{10}$$

5 APPLICATIONS

Assuming non-rotating NSs we calculate the sequences of equipotential contours of tori with cusp that provide the best matches to data of the individual sources. This can be done for the following 9 sources - 4U 1608-52, 4U 1636-53, 4U 1735-44, 4U 1915-05, IGR J17191-2821, GX 17+2, Sco X-1, Cir X-1 and XTE J1807.4-294. For these sources we find good agreement between the model and the data. In each case there is $0.5 < \chi^2/\text{d.o.f.} \lesssim 2$. We note that these sources span the approximate range of $\nu_L \in (200,\ 900)$Hz and include the atoll source 4U 1915-05 which itself covers a large range of frequencies, $\nu_L \in (200,\ 800)$Hz. We plot the relevant sequences of equipotential contours as well as the best data fits in Figures 4–6. These data fits are compared to the best fits obtained for the RP model. In all these sources the CT model matches the observed trend better than is done by the RP model. For the sake of clarity we also compare the relevant values of the torus thickness β to the exact values corresponding to the critical cusp torus configuration (see Török et al., 2016a for details). This is done in panels c) of Figures 4–6.

For the other 5 sources - 4U 1728-34, 4U 0614+09, 4U 1820-30, GX 340+0 and GX 5-1 - we cannot fit the data due to the model limitations discussed by Török et al. (2016a). For each of the 14 considered sources we compare the data and relation (9) for $\mathcal{B} = 0.8$. The resulting best fits are shown in Figure 7 along with the best fits obtained for the RP model. We furthermore perform fitting by relation (9) assuming $\mathcal{B}$ as a free parameter. In such case relation (9) matches the data in each of the 14 sources. This finding is illustrated in Figure 8.

The above mentioned outcomes of data fitting are summarized in Tables 5 and 6.

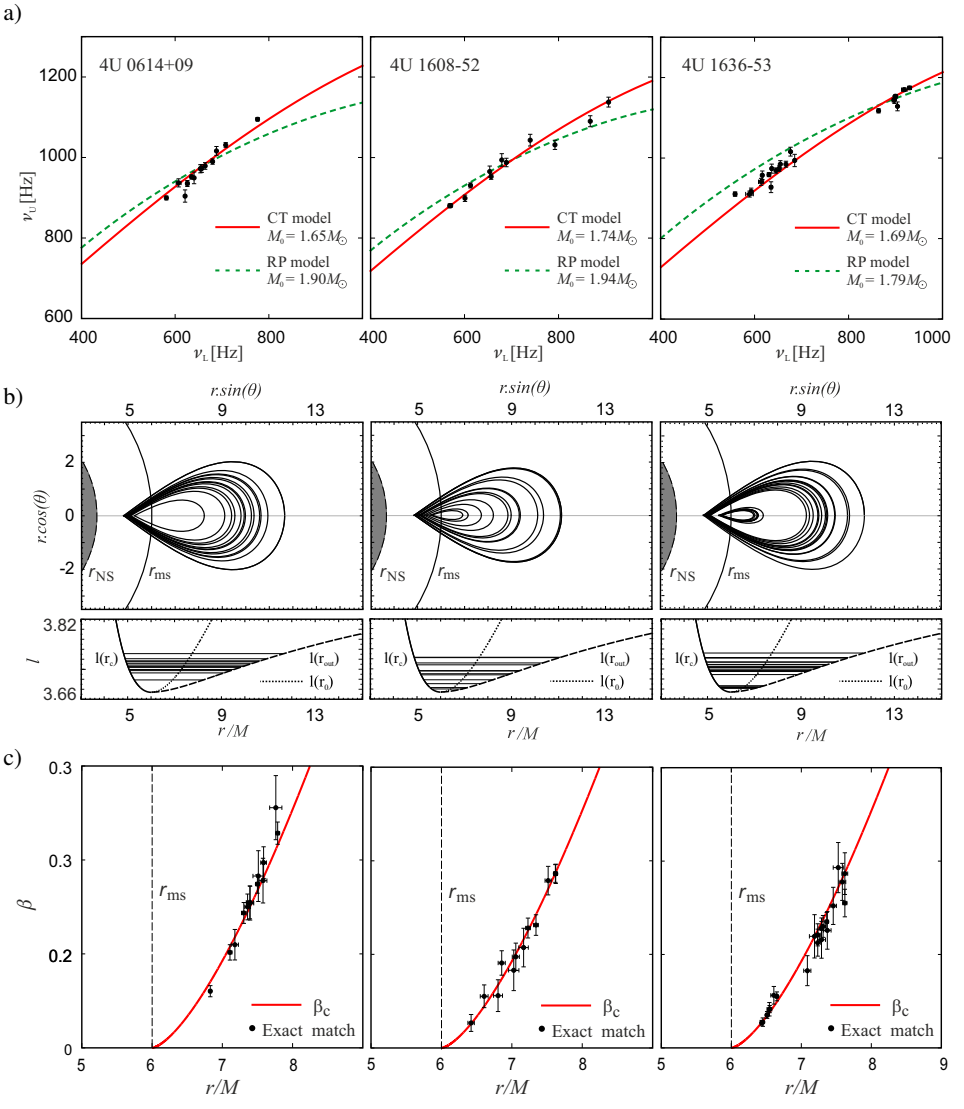

Figure 4. A comparison between the results obtained for the CT and the RP model. We consider here the three following sources - 4U 1608-52, 4U 1636-53 and 4U 1735-44. a) A sequence of tori with a cusp corresponding to a one-parametric data fit ($j = 0$). The bottom sub-panel always indicates the angular momentum behaviour along with the positions of the torus centre r_0 and both the inner and outer edge, r_c and r_{out}. b) The corresponding frequency relation plotted together with the datapoints. We also present the best fit implied by the RP model ($j = 0$). c) A consideration of the β and r combinations that exactly match the individual datapoints for the two chosen combinations of mass and angular momentum (see the paper of Török et al., 2016a). The red line denotes the numerically calculated CT model relation.

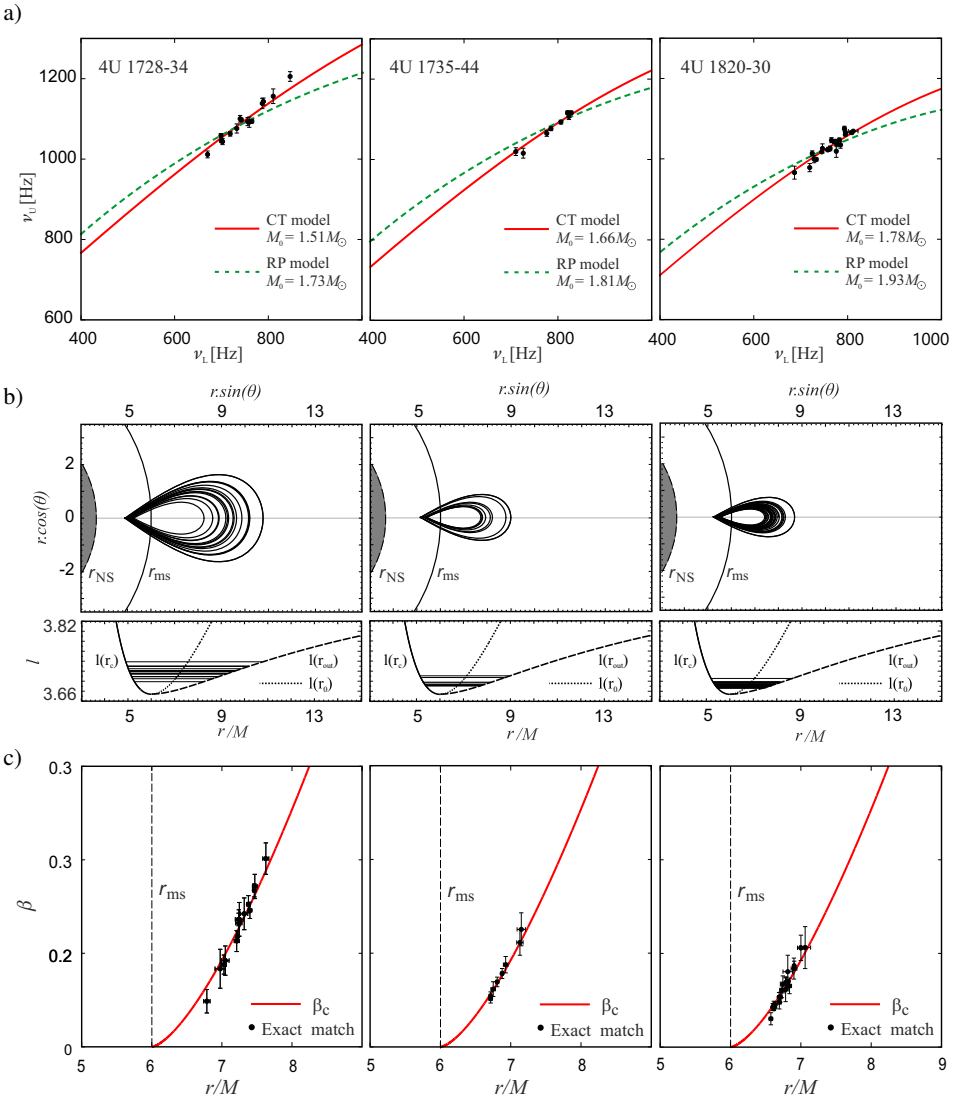

Figure 5. A comparison between the results obtained for the CT and the RP model. We consider here the three following sources - 4U 1728-34, 4U 1735-44 and 4U 1820-30. a) A sequence of tori with a cusp corresponding to a one-parametric data fit ($j = 0$). The bottom sub-panel always indicates the angular momentum behaviour along with the positions of the torus centre r_0 and both the inner and outer edge, r_c and r_{out}. b) The corresponding frequency relation plotted together with the datapoints. We also present the best fit implied by the RP model ($j = 0$). c) A consideration of the β and r combinations that exactly match the individual datapoints for the two chosen combinations of mass and angular momentum (see the paper of Török et al., 2016a). The red line denotes the numerically calculated CT model relation.

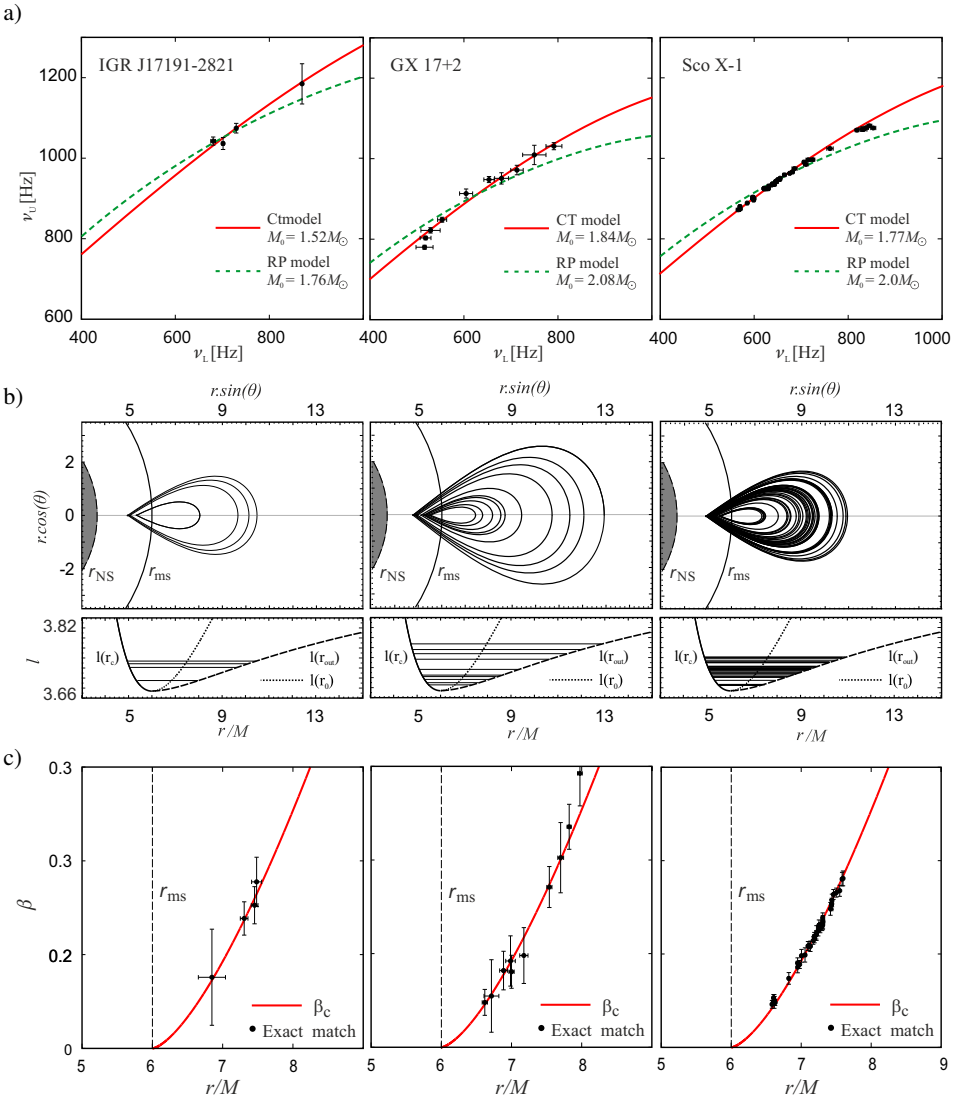

Figure 6. A comparison between the results obtained for the CT and the RP model. We consider here the three following sources - IGR J17191-2821, GX 17+2 and Sco X-1. a) A sequence of tori with a cusp corresponding to a one-parametric data fit ($j = 0$). The bottom sub-panel always indicates the angular momentum behaviour along with the positions of the torus centre r_0 and both the inner and outer edge, r_c and r_{out}. b) The corresponding frequency relation plotted together with the datapoints. We also present the best fit implied by the RP model ($j = 0$). c) A consideration of the β and r combinations that exactly match the individual datapoints for the two chosen combinations of mass and angular momentum (see the paper of Török et al., 2016a). The red line denotes the numerically calculated CT model relation.

Table 5. Parameters obtained through data matching - RP model and CT model.

Source No./ Type[a]	Name	$\frac{M_{\rm RP}}{M_\odot}$	$\frac{\chi^2_{\rm RP}}{d.o.f.}$	$\frac{M_{\rm CUSP}}{M_\odot}$	$\frac{\chi^2_{\rm CUSP}}{d.o.f.}$	Data-points
1/A	4U 1608-52	1.94	10.1	$1.74^{\pm 0.01}$	1.9	12
2/A	4U 1636-53	1.79	17.4	$1.69^{\pm 0.01}$	3.4	22
3/A	4U 1735-44	1.81	5.1	$1.66^{\pm 0.01}$	1.4	8
4/A	4U 1915-05	2.09	28.6	–[a]	–[a]	5
5/A	IGR J17191-2821	1.76	0.6	$1.52^{\pm 0.02}$	0.6	4
6/Z	GX 17+2	2.08	5.5	$1.83^{\pm 0.02}$	0.9	10
7/Z	Sco X-1	2.0	24.2	$1.76^{\pm 0.01}$	2.3	39
8/Z	Cir X-1	2.23	1.3	–[a]	–[a]	11
9/P	XTE J1807.4-294	3.27	1.4	–[a]	–[a]	7
10/A	4U 1728-34	1.74	5.7	$1.51^{\pm 0.01}$	2.8	15
11/A	4U 0614+09	1.90	14.7	$1.65^{\pm 0.01}$	3.4	13
12/A	4U 1820-30	1.93	24.2	$1.78^{\pm 0.01}$	6.4	23
13/Z	GX 340+0	2.07	1.8	–[a]	–[a]	12
14/Z	GX 5-1	2.13	3.1	–[a]	–[a]	21

[a] The observed frequencies extend below the expected range of physical applicability of the CT model discussed by Török et al. (2016a).

Table 6. Parameters obtained through data matching - relation (9) in its one- and two- parametric form.

Source No./Type	Name	$\mathcal{M}$	$\frac{\chi^2}{d.o.f.}$	$\mathcal{M}(\mathcal{B})$	$\mathcal{B}$	$\frac{\chi^2_{\mathcal{M}(\mathcal{B})}}{d.o.f.}$	Data-points
1/A	4U 1608-52	$1.80^{\pm 0.01}$	1.6	$1.79^{\pm 0.04}$	$0.79^{\pm 0.03}$	1.7	12
2/A	4U 1636-53	$1.70^{\pm 0.01}$	2.0	$1.70^{\pm 0.01}$	$0.8^{\pm 0.01}$	2.1	22
3/A	4U 1735-44	$1.69^{\pm 0.01}$	2.1	$1.48^{\pm 0.10}$	$0.61^{\pm 0.06}$	1.0	8
4/A	4U 1915-05	$1.58^{\pm 0.03}$	0.8	$1.65^{\pm 0.03}$	$0.82^{\pm 0.01}$	0.2	5
5/A	IGR J17191	$1.58^{\pm 0.02}$	0.6	$1.63^{\pm 0.20}$	$0.85^{\pm 0.2}$	0.8	4
6/Z	GX 17+2	$1.89^{\pm 0.02}$	1.2	$1.77^{\pm 0.07}$	$0.72^{\pm 0.04}$	0.8	10
7/Z	Sco X-1	$1.82^{\pm 0.01}$	1.0	$1.81^{\pm 0.01}$	$0.8^{\pm 0.01}$	1.0	39
8/Z	Cir X-1	$0.74^{\pm 0.10}$	1.2	$1.42^{\pm 0.5}$	$0.89^{\pm 0.06}$	1.1	11
9/P	XTE J1807.4	$2.61^{\pm 0.11}$	0.8	$2.85^{\pm 0.25}$	$0.86^{\pm 0.07}$	0.8	7
10/A	4U 1728-34	$1.57^{\pm 0.01}$	3.2	$1.35^{\pm 0.12}$	$0.65^{\pm 0.06}$	2.5	15
11/A	4U 0614+09	$1.71^{\pm 0.02}$	5.1	$1.39^{\pm 0.06}$	$0.62^{\pm 0.02}$	1.1	13
12/A	4U 1820-30	$1.81^{\pm 0.01}$	9.3	$1.53^{\pm 0.07}$	$0.58^{\pm 0.03}$	3.2	23
13/Z	GX 340+0	$1.62^{\pm 0.08}$	4.2	$2.23^{\pm 0.10}$	$1.10^{\pm 0.08}$	1.6	12
14/Z	GX 5-1	$1.65^{\pm 0.10}$	16.7	$2.31^{\pm 0.04}$	$1.11^{\pm 0.02}$	1.5	21

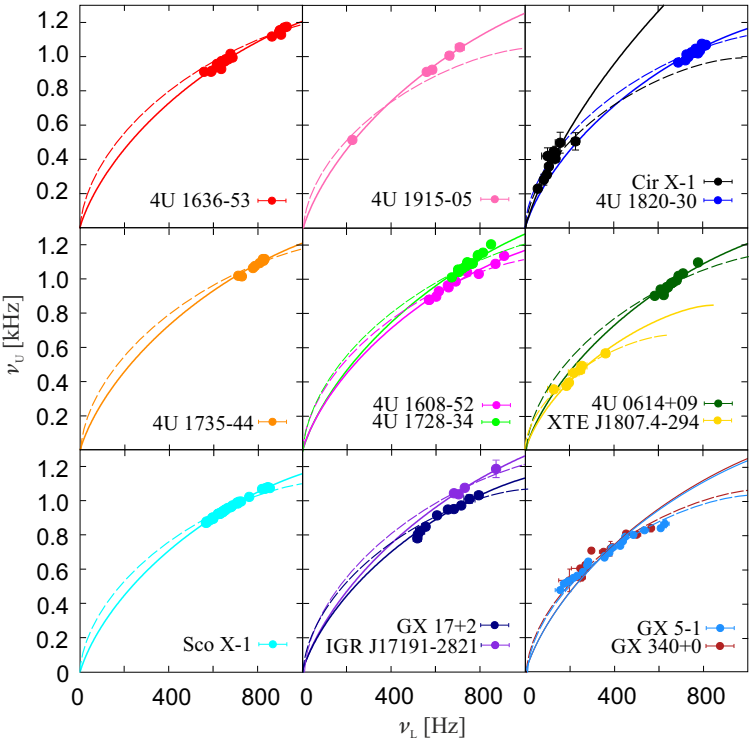

Figure 7. The best fits obtained using relation (9) for $\mathcal{B} = 0.8$ in each of the 14 sources (the solid lines). The best fits carried out for the RP model are shown as well (the dashed lines).

6 DISCUSSION AND CONCLUSIONS

We suggest that relation (9) is likely related to global modes of orbital motion (see the studies of Rezzolla et al., 2003; Abramowicz et al., 2006; Šrámková et al., 2007; Ingram and Done, 2010; Fragile et al., 2016; Török et al., 2016a; Mishra et al., 2017; Parthasarathy et al., 2017; de Avellar et al., 2017 and references therein).

We conclude that for $\mathcal{B} = 0.8$ the CT model as well as relation (9) well reproduce the data of 9 sources. When $\mathcal{B}$ is considered as a free parameter, we obtain good fits for each of the 14 considered sources. Within the CT model framework, larger deviations from the case of $\mathcal{B} = 0.8$ can have a direct physical interpretation. They may be caused by further non-geodesic effects acting on the torus formation induced by, e.g., the influence of magnetic field. This would agree with the general interpretation, in which the $\mathcal{M}$ parameter represents the main parameter which reflects the spacetime geometry given by the NS mass and spin, while the $\mathcal{B}$ parameter reflects the additional stable factors.

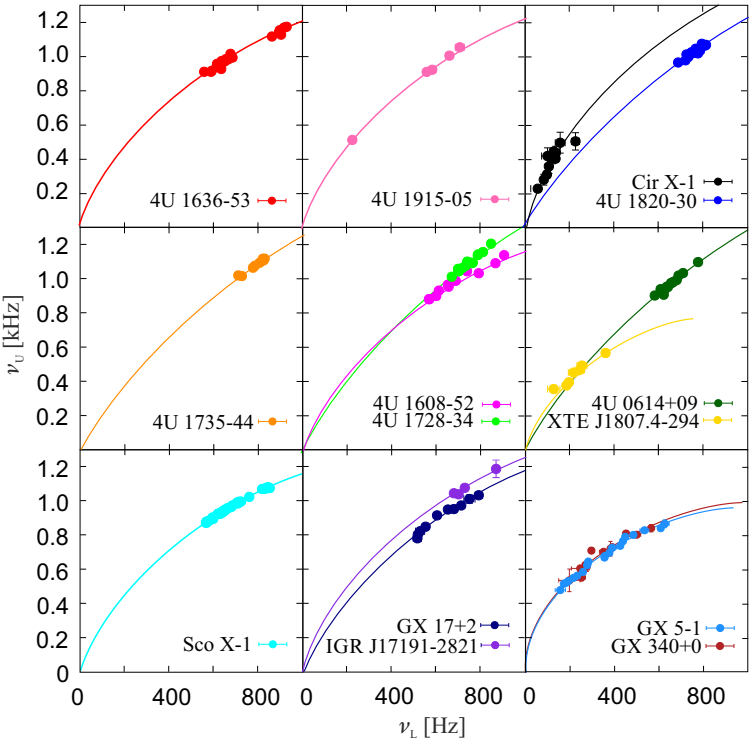

Figure 8. The best fits obtained using relation (9) while assuming $\mathcal{B}$ as a free parameter in each of the 14 sources.

ACKNOWLEDGEMENTS

We would like to acknowledge the Czech Science Foundation grant No. 17-16287S, the INTER-EXCELLENCE project No. LTI17018 aimed to support collaboration between the Silesian University in Opava (SU) and the Astronomical Institute in Prague (ASU), and the internal SU grant No. SGS/15/2016. We are grateful to Marek Abramowicz (SU) and Omer Blaes (University of California in Santa Barbara - UCSB) for useful discussions. Last but not least we would like to acknowledge the hospitality of UCSB and to express our thanks to concierges of Mlýnská hotel in Uherské Hradiště, Czech Republic for their participation in organizing frequent workshops of SU and ASU.

REFERENCES

Abramowicz, M. A., Barret, D., Bursa, M., Horák, J., Kluźniak, W., Rebusco, P. and Török, G. (2005a), A note on the slope-shift anticorrelation in the neutron star kHz QPOs data, in S. Hledík

and Z. Stuchlík, editors, *RAGtime 6/7: Workshops on black holes and neutron stars*, pp. 1–9.

Abramowicz, M. A., Barret, D., Bursa, M., Horák, J., Kluźniak, W., Rebusco, P. and Török, G. (2005b), The correlations and anticorrelations in QPO data, *Astronomische Nachrichten*, **326**, pp. 864–866, arXiv: astro-ph/0510462.

Abramowicz, M. A., Blaes, O. M., Horák, J., Kluźniak, W. and Rebusco, P. (2006), Epicyclic oscillations of fluid bodies: II. Strong gravity, *Classical and Quantum Gravity*, **23**, pp. 1689–1696, arXiv: astro-ph/0511375.

Abramowicz, M. A., Karas, V., Kluźniak, W., Lee, W. H. and Rebusco, P. (2003), Non-Linear Resonance in Nearly Geodesic Motion in Low-Mass X-Ray Binaries, *PASJ*, **55**, pp. 467–466, arXiv: astro-ph/0302183.

Alpar, M. A. and Shaham, J. (1985), Is GX5 - 1 a millisecond pulsar?, *Nature*, **316**, pp. 239–241.

Altamirano, D., Linares, M., Patruno, A., Degenaar, N., Wijnands, R., Klein-Wolt, M., van der Klis, M., Markwardt, C. and Swank, J. (2010), Type I X-ray bursts, burst oscillations and kHz quasi-periodic oscillations in the neutron star system IGRJ17191-2821, *MNRAS*, **401**, pp. 223–230, arXiv: 0908.4039.

Barret, D., Olive, J.-F. and Miller, M. C. (2005a), An abrupt drop in the coherence of the lower kHz quasi-periodic oscillations in 4U 1636-536, *MNRAS*, **361**, pp. 855–860, arXiv: astro-ph/0505402.

Barret, D., Olive, J.-F. and Miller, M. C. (2005b), Drop of coherence of the lower kilo-Hz QPO in neutron stars: Is there a link with the innermost stable circular orbit?, *Astronomische Nachrichten*, **326**, pp. 808–811, arXiv: astro-ph/0510094.

Barret, D., Olive, J.-F. and Miller, M. C. (2006), The coherence of kilohertz quasi-periodic oscillations in the X-rays from accreting neutron stars, *MNRAS*, **370**, pp. 1140–1146, arXiv: astro-ph/0605486.

Boirin, L., Barret, D., Olive, J. F., Bloser, P. F. and Grindlay, J. E. (2000), Low and high frequency quasi-periodic oscillations in 4U1915-05, *Astronomy and Astrophysics*, **361**, pp. 121–138, arXiv: astro-ph/0007071.

Boutloukos, S., van der Klis, M., Altamirano, D., Klein-Wolt, M., Wijnands, R., Jonker, P. G. and Fender, R. P. (2006), Discovery of Twin kHz QPOs in the Peculiar X-Ray Binary Circinus X-1, *APJ*, **653**, pp. 1435–1444, arXiv: astro-ph/0608089.

Bradt, H. V., Rothschild, R. E. and Swank, J. H. (1993), X-ray timing explorer mission, *ApJ Supp.*, **97**, pp. 355–360.

Bursa, M. (2005), High-frequency QPOs in GRO J1655-40: Constraints on resonance models by spectral fits, in S. Hledík and Z. Stuchlík, editors, *RAGtime 6/7: Workshops on black holes and neutron stars*, pp. 39–45.

de Avellar, M. G., Porth, O., Younsi, Z. and Rezzolla, L. (2017), The kilo Hertz quasi-periodic oscillations in neutron star low-mass X-ray binaries as tori oscillation modes. I, *ArXiv e-prints*, arXiv: 1709.07706.

Fragile, P. C., Straub, O. and Blaes, O. (2016), High-frequency and type-C QPOs from oscillating, precessing hot, thick flow, *MNRAS*, **461**, pp. 1356–1362, arXiv: 1602.08082.

Homan, J., van der Klis, M., Jonker, P. G., Wijnands, R., Kuulkers, E., Méndez, M. and Lewin, W. H. G. (2002), RXTE Observations of the Neutron Star Low-Mass X-Ray Binary GX 17+2: Correlated X-Ray Spectral and Timing Behavior, *The Astrophysical Journal*, **568**, pp. 878–900, arXiv: astro-ph/0104323.

Ingram, A. and Done, C. (2010), A physical interpretation of the variability power spectral components in accreting neutron stars, *MNRAS*, **405**, pp. 2447–2452, arXiv: 0907.5485.

Jonker, P. G., van der Klis, M., Homan, J., Méndez, M., Lewin, W. H. G., Wijnands, R. and Zhang,

W. (2002), Low- and high-frequency variability as a function of spectral properties in the bright X-ray binary GX 5-1, *MNRAS*, **333**, pp. 665–678, arXiv: astro-ph/0202420.

Jonker, P. G., van der Klis, M., Wijnands, R., Homan, J., van Paradijs, J., Méndez, M., Ford, E. C., Kuulkers, E. and Lamb, F. K. (2000), The Power Spectral Properties of the Z Source GX 340+0, *The Astrophysical Journal*, **537**, pp. 374–386, arXiv: astro-ph/0002022.

Kato, S. (2001), Basic Properties of Thin-Disk Oscillations, *PASJ*, **53**, pp. 1–24.

Kluźniak, W. and Abramowicz, M. A. (2001), The physics of kHz QPOs—strong gravity's coupled anharmonic oscillators, *ArXiv Astrophysics e-prints*, arXiv: astro-ph/0105057.

Kluźniak, W., Abramowicz, M. A., Kato, S., Lee, W. H. and Stergioulas, N. (2004), Nonlinear Resonance in the Accretion Disk of a Millisecond Pulsar, *AJ*, **603**, pp. L89–L92, arXiv: astro-ph/0308035.

Kluzniak, W., Michelson, P. and Wagoner, R. V. (1990), Determining the properties of accretion-gap neutron stars, *ApJ*, **358**, pp. 538–544.

Kluzniak, W. and Wagoner, R. V. (1985), Evolution of the innermost stable orbits around accreting neutron stars, *ApJ*, **297**, pp. 548–554.

Lamb, F. K., Shibazaki, N., Alpar, M. A. and Shaham, J. (1985), Quasi-periodic oscillations in bright galactic-bulge X-ray sources, *Nature*, **317**, pp. 681–687.

Lewin, W. H. G., van Paradijs, J. and van den Heuvel, E. P. J. (1997), *X-ray Binaries*, Cambridge University Press.

Lin, Y.-F., Boutelier, M., Barret, D. and Zhang, S.-N. (2011), Studying Frequency Relationships of Kilohertz Quasi-periodic Oscillations for 4U 1636-53 and Sco X-1: Observations Confront Theories, *The Astrophysical Journal*, **726**, 74, arXiv: 1010.6198.

Linares, M., van der Klis, M., Altamirano, D. and Markwardt, C. B. (2005), Discovery of Kilohertz Quasi-periodic Oscillations and Shifted Frequency Correlations in the Accreting Millisecond Pulsar XTE J1807-294, *The Astrophysical Journal*, **634**, pp. 1250–1260, arXiv: astro-ph/0509011.

Miller, M. C., Lamb, F. K. and Psaltis, D. (1998), Sonic-Point Model of Kilohertz Quasi-periodic Brightness Oscillations in Low-Mass X-Ray Binaries, *AJ*, **508**, pp. 791–830, arXiv: astro-ph/9609157.

Mishra, B., Vincent, F. H., Manousakis, A., Fragile, P. C., Paumard, T. and Kluźniak, W. (2017), Quasi-periodic oscillations from relativistic ray-traced hydrodynamical tori, *MNRAS*, **467**, pp. 4036–4049.

Mukhopadhyay, B. (2009), Higher-Order Nonlinearity in Accretion Disks: Quasi-Periodic Oscillations of Black Hole and Neutron Star Sources and Their Spin, *AJ*, **694**, pp. 387–395, arXiv: 0811.2033.

Parthasarathy, V., Kluzniak, W. and Cemeljic, M. (2017), MHD simulations of oscillating cusp-filling tori around neutron stars – missing upper kHz QPO, *ArXiv e-prints*, arXiv: 1703.05036.

Pétri, J. (2005), An explanation for the kHz-QPO twin peaks separation in slow and fast rotators, *A&A*, **439**, pp. L27–L30, arXiv: astro-ph/0507167.

Psaltis, D., Méndez, M., Wijnands, R., Homan, J., Jonker, P. G., van der Klis, M., Lamb, F. K., Kuulkers, E., van Paradijs, J. and Lewin, W. H. G. (1998), The Beat-Frequency Interpretation of Kilohertz Quasi-periodic Oscillations in Neutron Star Low-Mass X-Ray Binaries, *ApJ Lett.*, **501**, pp. L95–L99, arXiv: astro-ph/9805084.

Psaltis, D., Wijnands, R., Homan, J., Jonker, P. G., van der Klis, M., Miller, M. C., Lamb, F. K., Kuulkers, E., van Paradijs, J. and Lewin, W. H. G. (1999), On the Magnetospheric Beat-Frequency and Lense-Thirring Interpretations of the Horizontal-Branch Oscillation in the Z Sources, *AJ*, **520**, pp. 763–775, arXiv: astro-ph/9903105.

Rezzolla, L., Yoshida, S. and Zanotti, O. (2003), Oscillations of vertically integrated relativistic

tori - I. Axisymmetric modes in a Schwarzschild space-time, *MNRAS*, **344**, pp. 978–992, arXiv: astro-ph/0307488.

Šrámková, E., Torkelsson, U. and Abramowicz, M. A. (2007), Oscillations of tori in the pseudo-Newtonian potential, *A&A*, **467**, pp. 641–646, arXiv: 0802.3856.

Stella, L. and Vietri, M. (2001), Quasi-Periodic Oscillations from Low-Mass X-ray Binaries and Strong Field Gravity, in R. Giacconi, S. Serio and L. Stella, editors, *X-ray Astronomy 2000*, volume 234 of *Astronomical Society of the Pacific Conference Series*, p. 213.

Straub, O. and Šrámková, E. (2009), Epicyclic oscillations of non-slender fluid tori around Kerr black holes, *Classical and Quantum Gravity*, **26**(5), 055011, arXiv: 0901.1635.

Stuchlík, Z., Kotrlová, A. and Török, G. (2013), Multi-resonance orbital model of high-frequency quasi-periodic oscillations: possible high-precision determination of black hole and neutron star spin, *A&A*, **552**, A10, arXiv: 1305.3552.

Titarchuk, L. and Wood, K. (2002), On the Low and High Frequency Correlation in Quasi-periodic Oscillations among White Dwarf, Neutron Star, and Black Hole Binaries, *AJ*, **577**, pp. L23–L26, arXiv: astro-ph/0208212.

Török, G., Bakala, P., Šrámková, E., Stuchlík, Z. and Urbanec, M. (2010), On Mass Constraints Implied by the Relativistic Precession Model of Twin-peak Quasi-periodic Oscillations in Circinus X-1, *AJ*, **714**, pp. 748–757, arXiv: 1008.0088.

Török, G., Bakala, P., Šrámková, E., Stuchlík, Z., Urbanec, M. and Goluchová, K. (2012), Mass-Angular-momentum Relations Implied by Models of Twin Peak Quasi-periodic Oscillations, *ApJ*, **760**, 138, arXiv: 1408.4220.

Török, G., Goluchová, K., Horák, J., Šrámková, E., Urbanec, M., Pecháček, T. and Bakala, P. (2016a), Twin peak quasi-periodic oscillations as signature of oscillating cusp torus, *MNRAS*, **457**, pp. L19–L23, arXiv: 1512.03841.

Török, G., Goluchová, K., Urbanec, M., Šrámková, E., Adámek, K., Urbancová, G., Pecháček, T., Bakala, P., Stuchlík, Z., Horák, J. and Juryšek, J. (2016b), Constraining Models of Twin-Peak Quasi-periodic Oscillations with Realistic Neutron Star Equations of State, *The Astrophysical Journal*, **833**, 273, arXiv: 1611.06087.

Török, G., Goluchová, K., Šrámková, E., Horák, J., Bakala, P. and Urbanec, M. (2017), On one-parametric formula relating the frequencies of twin-peak quasi-periodic oscillations, *ArXiv e-prints*, accepted for publication in MNRAS, arXiv: 1710.10901.

Čadež, A., Calvani, M. and Kostić, U. (2008), On the tidal evolution of the orbits of low-mass satellites around black holes, *A&A*, **487**, pp. 527–532, arXiv: 0809.1783.

van der Klis, M. (2006), *Rapid X-ray Variability*, pp. 39–112, Cambridge University Press.

van der Klis, M., Wijnands, R. A. D., Horne, K. and Chen, W. (1997), Kilohertz Quasi-Periodic Oscillation Peak Separation Is Not Constant in Scorpius X-1, *APJL*, **481**, pp. L97–L100, arXiv: astro-ph/9703025.

Wagoner, R. V., Silbergleit, A. S. and Ortega-Rodríguez, M. (2001), "Stable" Quasi-periodic Oscillations and Black Hole Properties from Diskoseismology, *AJ*, **559**, pp. L25–L28, arXiv: astro-ph/0107168.

Zhang, C. (2004), The MHD Alfven wave oscillation model of kHz Quasi Periodic Oscillations of Accreting X-ray binaries, *A&A*, **423**, pp. 401–404, arXiv: astro-ph/0402028.

Zhang, C. M., Yin, H. X., Zhao, Y. H., Zhang, F. and Song, L. M. (2006), The correlations between the twin kHz quasi-periodic oscillation frequencies of low-mass X-ray binaries, *MNRAS*, **366**, pp. 1373–1377, arXiv: astro-ph/0601318.